Effects of Magnetic Islands Produced by External Perturbation Fields in the Tohoku University Heliac

Sumio KITAJIMA, Junya SATO, Keiichi ISHII, Takanori AMBO, Mamoru KANNO, Atsushi OKAMOTO, Mamiko SASAO, Shigeru INAGAKI[1)], Masakazu TAKAYAMA[2)], Kiyohiko NISHIMURA[3)], Yasuhiro SUZUKI[3)], Masayuki YOKOYAMA[3)] and Hiromi TAKAHASHI[3)]

Department of Quantum Science and Energy Engineering, Tohoku University, Sendai 980-8579, Japan

[1)]*Research Institute for Applied Mechanics Kyushu University 6-1 Kasuga-kouen, Kasuga, Fukuoka 816-8580, Japan*

[2)]*Akita Prefectural University, Honjyo, Akita 015-0055, Japan*

[3)]*National Institute for Fusion Science,322-6 Oroshi-cho, Toki 509-5292, Japan*

(Received 21 December 2009 / Accepted 9 April 2010)

Island effects on the plasma periphery due to the external perturbation fields in the Tohoku University Heliac (TU-Heliac) were surveyed. A fixed $m = 3$ magnetic island was produced by two pairs of external cusp field coils. The electron density decayed from the outer edge of the island after perturbation field application. Radial profiles of the electron temperature and plasma space potential in the island region revealed the magnetic island structure. The radial electric field at the inner edge of the island increased after perturbation field application. The positions of local maxima in the plasma space potential profile were in good agreement with the position of the $n/m = 5/3$ rational surface. The potential profile in the island grew with the perturbation field strength. The full width at half maximum of the potential profile depended on the square root of the perturbation field coil current.

Keywords: stellarator, heliac, magnetic island, poloidal rotation, perturbation field, electrode bias

DOI: 10.1585/pfr.5.S2041

1. Introduction

Study of magnetic island effects on a plasma periphery is important for realizing a fusion reactor, because it is expected to lead to advanced control methods for edge plasma in the reactor. It is particularly important to know the island effects on the plasma periphery in order to control the edge-localized mode in ITER [1]. For the research on island effects in edge plasma, the Tohoku University Heliac (TU-Heliac) has the following advantages: (1) The rotational transform profile can be changed by selecting the ratio of coil currents: (2) island formation can be controlled by externally perturbation field coils: and (3) the radial electric field and particle transport can be controlled externally by electrode biasing [2]. In the TU-Heliac, an improved mode transition has been triggered by electrode biasing using a hot cathode made of LaB_6. The driving force for a plasma poloidal rotation $\boldsymbol{J} \times \boldsymbol{B}$ was externally controlled, and the poloidal viscosity was successfully estimated from the external driving force [2, 3]. Therefore, electrode biasing has advantages for the formation of the radial electric field and making a flow in plasma surrounded by magnetic islands to study the island effect on plasma flow. In recent experiments, the ion viscosity in biased plasma with islands was roughly estimated. The result suggested that the poloidal viscosity increased with increasing magnetic island width [4]. Therefore, it is expected that plasma poloidal rotation will be driven by the poloidal rotation of the island [5].

It is important to understand the controllability of the poloidal viscosity by the external torque and the relationship between radial transport and island width utilizing the advantage that a Heliac device has the flexibility in configurations. The purpose of this experiment is to survey magnetic island development and the degradation of the plasma peripheral pressure or the degradation of radial transport during the application of an external magnetic perturbation.

2. Experimental Setup

2.1 TU-Heliac

The TU-Heliac is a four-period heliac (major radius, 0.48 m; average plasma radius, 0.07 m). The heliac configurations were produced by three sets of magnetic field coils: 32 toroidal field coils, a center conductor coil, and one pair of vertical field coils, as shown in Fig. 1. Three capacitor banks consisting of two-stage pulse-forming networks separately supplied coil currents of 10-ms flat top duration. The target plasma for the external perturbation fields was He plasma produced by low-frequency joule heating ($f = 18.8$ kHz, $P_{out} \sim 35$ kW). The joule heating power was supplied to one pair of poloidal coils wound

author's e-mail: sumio.kitajima@qse.tohoku.ac.jp

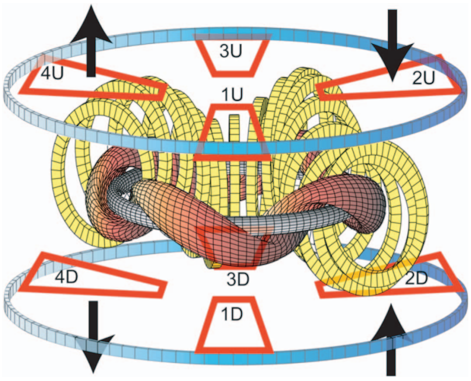

Fig. 1 Bird's eye-view of TU-Heliac. Four pairs of upper and lower external perturbation field coils are located at the toroidal angles $\phi = 0°$, $90°$, $180°$ and $270°$.

outside the toroidal coils. The vacuum vessel was filled with a fuel of neutral He gas and sealed from the evacuation system before every discharge. The electron density and temperature measured by a Langmuir probe (triple probe) were $\sim 1 \times 10^{18}\ \mathrm{m}^{-3}$ and $\sim 20\ \mathrm{eV}$, respectively, at the magnetic axis, and the magnetic field strength at the axis was 0.3 T.

2.2 External perturbation coils

In this experiment, we adopted a magnetic configuration that has a rational flux surface ($n/m = 5/3$) at $\rho \sim 0.5$ by selecting the coil current ratio. The rotational transform profile is shown in Fig. 2. We searched for an efficient setting for the perturbation coils for generating islands ($m = 3$). We chose four pairs of upper and lower external perturbation field coils located at the toroidal angles $\phi = 0°$, $90°$, $180°$ and $270°$ and generated a cusp field at each toroidal angle, as shown in Fig. 1. We have explored the possibility of the poloidal rotation of islands by changing the phase of each perturbation coil current [5]. In this experiment, to study the island structure located at fixed poloidal positions, we used only two pairs of external perturbation field coils at the toroidal angles $\phi = 90°$ and $270°$. Therefore, the $m = 3$ magnetic island did not rotate along the poloidal direction. We optimized the perturbation fields to resonate only the $n/m = 5/3$ rational surface. Slight effects of the other mode components ($n/m = 8/5$, $n/m = 12/7$) in the field remained in our configuration. An external perturbation field coil current I_{ex} of up to 3.6 kAT flowed in each coil producing the radial component of the perturbation field $B_r/B_0 = 5.7 \times 10^{-3}$ at the positions on the rational surface ($n/m = 5/3$) closest to the perturbation field coil. Here B_0 is the magnetic field strength at the magnetic axis. The magnetic surfaces at the toroidal angle $\phi = 0°$ are shown in Fig. 2. The perturbation field coil current I_{ex} was three times greater than that in the previous rotating island experiment [5].

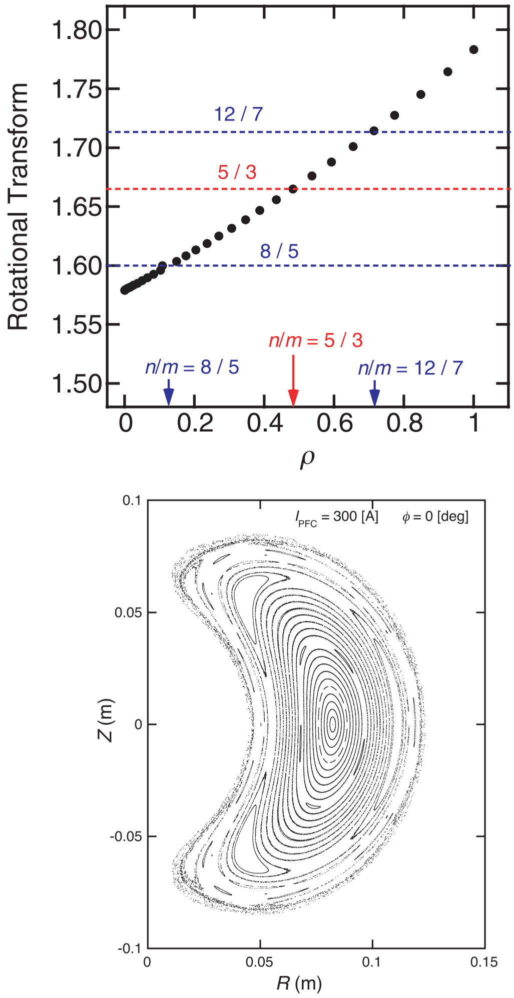

Fig. 2 Rotational transform profile and magnetic surfaces with $m = 3$ islands.

3. Experimental Results

3.1 Electron density profile

The typical time evolutions of plasma parameters at the O-point in the island are shown in Fig. 3. The electron density, electron temperature and space potential were measured by a high-speed triple probe [6, 7]. An external perturbation field was added at $t = 5$ ms. The perturbation coil current I_{ex} increased exponentially with time because of the inductive component of the perturbation field coils. After the perturbation field was applied, gradual changes appeared in electron density, electron temperature and fluctuation signals in the ion saturation current and the floating potential.

We measured the radial profiles of electron density by scanning the triple probe on the equatorial plane from the low-field side in the magnetic configuration shown in Fig. 2. We can measure the density profile across the O-point in the $m = 3$ island. A two-dimensional plot of the radial profiles is shown in Fig. 4, in which the vertical and the horizontal axes indicate the radial position and the duration, respectively, of plasma production ($0 < t < 10$ ms).

The rational surface ($n/m = 5/3$), the magnetic axis, and the lasted closed flux surface (LCFS) are located at R = 82, 112, and 125 mm, respectively. The $m = 3$ island was located at 109 mm < R < 114.5 mm. R = 0 mm indicates the center of the cross section of the center conductor coil. The electron density decreased at the outer edge of the island after the perturbation field was applied. An external perturbation field was added at t = 5 ms. However, Fig. 5 shows that 75% of the electron density before perturbation field application remained in the island region. Before perturbation field application we can observe a slight density flattening in the island region in Fig. 5. One of the reasons is the natural island made by the error field without the external perturbation fields.

3.2 Electron temperature and space potential profile

Figure 6 shows the radial profile of the electron temperature and plasma space potential. Both had local maxima in the island region (109 mm < R < 114.5 mm) after perturbation field application. The radial electric field at the inner edge of the island (109 mm < R < 112 mm) increased after perturbation field application. In contrast to the density profile the potential profile tended to have the same value at the inner and outer edges of the island because of a short-circuit in the magnetic lines of force.

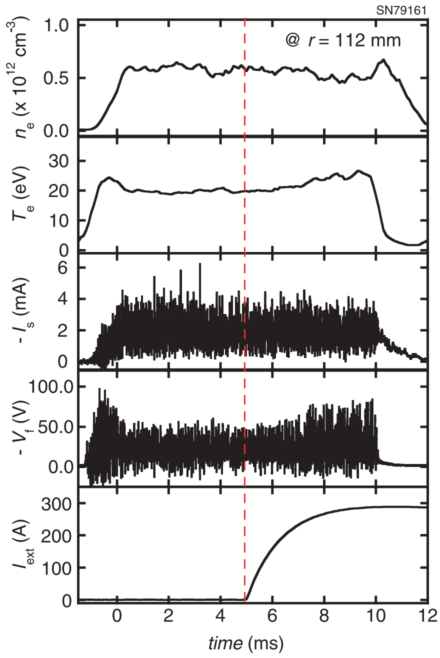

Fig. 3 The typical time evolution of the electron density, electron temperature, space potential, fluctuation signals in the ion saturation current and the floating potential and the external perturbation coil current.

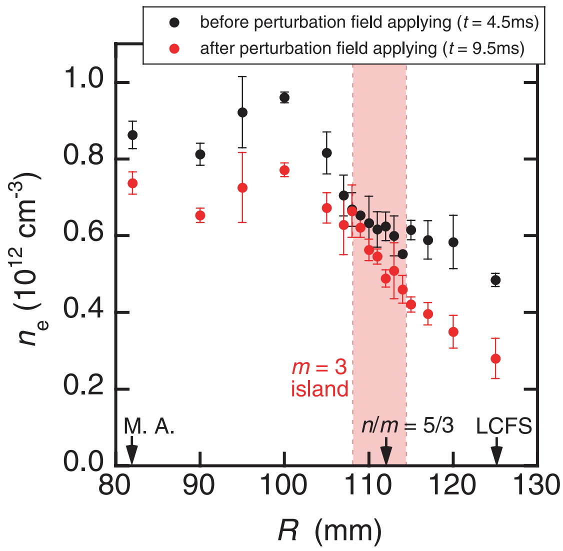

Fig. 5 Radial profile of electron density. The $m = 3$ island is located in the region 109 mm < R < 114.5 mm.

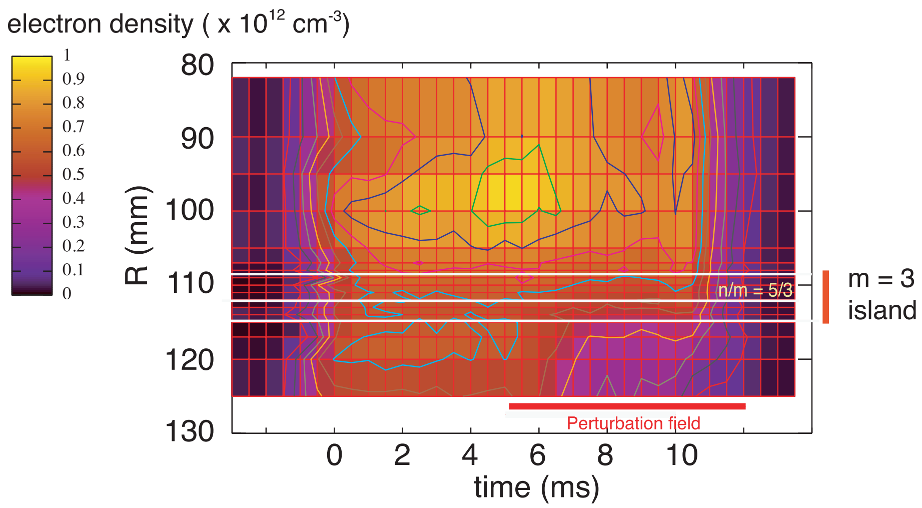

Fig. 4 Radial profiles of the electron density. Vertical and the horizontal axes indicate the radial position and the duration, respectively, of plasma production (0 < t < 10 ms).

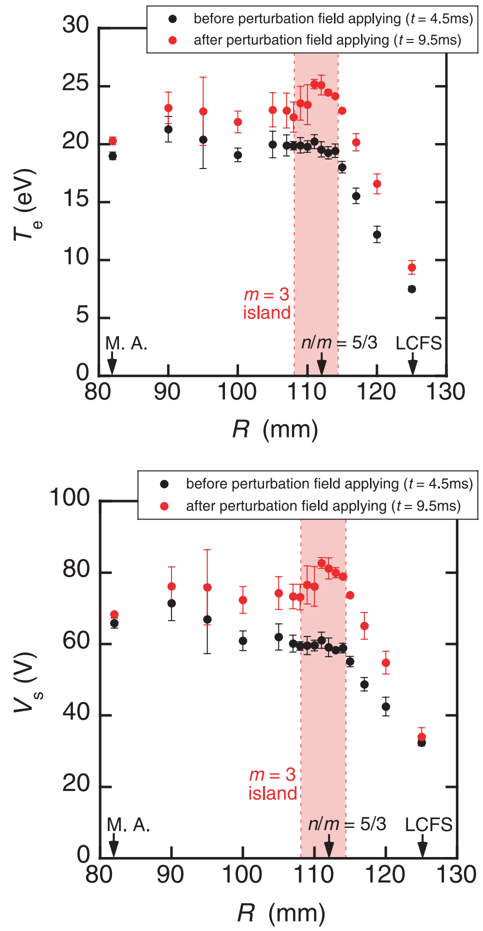

Fig. 6 Radial profiles of electron temperature and plasma space potential.

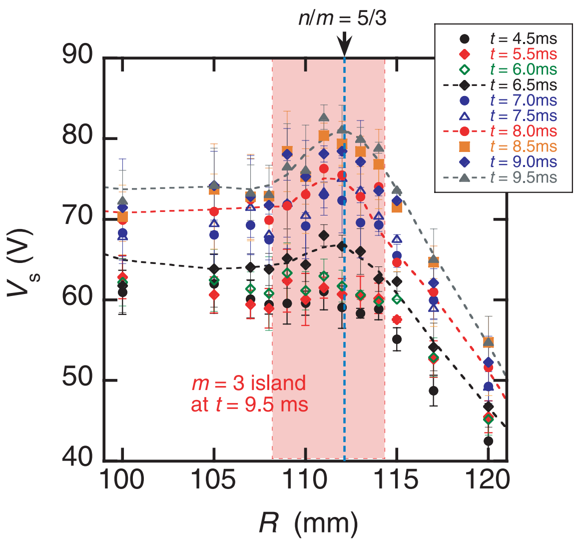

Fig. 7 Radial profiles of the plasma space potential. Perturbation field was applied at t = 5 ms.

A detailed time evolution of the radial profile of the plasma space potential is shown in Fig. 7. The profile spread with the increase in the perturbation field. The perturbation coil current I_{ex} increased depending on time. The positions of the peaks in the profiles are in good agreement with the position of the n/m = 5/3 rational surface.

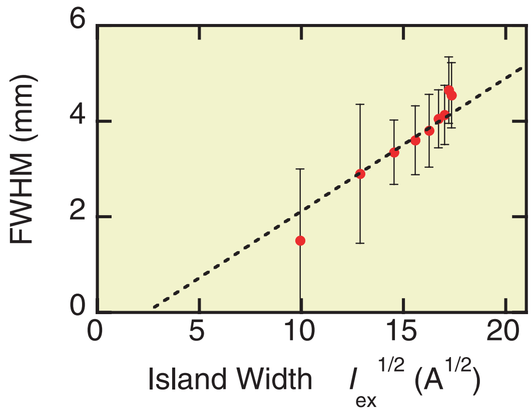

Fig. 8 Relationship between the full width at half maximum (FWHM) of the potential profile and the external perturbation coil current.

The full width at half maximum (FWHM) of the potential profiles in Fig. 7 is shown in Fig. 8. The FWHM was estimated from a profile that was modified by subtracting the base part from the original potential value in the island region.

Figure 8 clearly shows that the full width at half maximum (FWHM) of the potential profile depends on the square root of the perturbation field coil current I_{ex}. It is considered that island width is linearly proportional to the square root of the radial component in the perturbation field. These results provide information about requirement of the strength of the perturbation field, and the development of the island structure followed the time-variant perturbation field.

4. Summary

We surveyed the island effects on the plasma periphery caused by the external perturbation fields in the TU-Heliac. We produced a fixed m = 3 magnetic island (not rotating) by two pairs of cusp field coils. The electron density decayed from the outer edge of the island after perturbation field application, which suggests the degradation of radial transport. Radial profiles of the electron temperature and plasma space potential in the island region showed the magnetic island's structure, revealing that the potential was constant along the magnetic field lines. The radial electric field at the inner edge of the island increased after perturbation field application. The potential profile in the island grew with the square root of the perturbation field strength.

This work was supported by the LHD Joint Planning Research program at National Institute for Fusion Science.

[1] T. E. Evans *et al.*, Phys. Rev. Lett. **92**, 235003 (2004).
[2] S. Kitajima *et al.*, Nucl. Fusion **46**, 200 (2006).
[3] H. Takahashi *et al.*, Plasma Phys. Control. Fusion **48**, 39 (2006).

[4] S. Kitajima *et al*., Fusion Sci. Technol. **50**, 201 (2006).
[5] S. Kitajima *et al.*, Plasma Fusion Res. **3**, S1027 (2008).
[6] Y. Tanaka *et al*., Plasma Fusion Res. **2**, S1019 (2007).
[7] Y. Tanaka *et al*., Plasma Phys. Control. Fusion **48**, A285 (2006).